Inherent structures in polyatomic liquids: Simulation for Si_2F_6

Thomas A. Weber
Division of Advanced Scientific Computing, National Science Foundation, Washington, DC 20550

Frank H. Stillinger
AT&T Bell Laboratories, Murray Hill, New Jersey 07974

(Received 25 October 1990; accepted 22 May 1991)

A molecular dynamics study has been carried out on a model for the polyatomic liquid Si_2F_6. A wide range of temperatures was examined, as well as a 19% density variation. Transferrable two-atom and three-atom interaction functions were combined to represent the system potential energy, and to allow for the possibility of chemical rearrangements. It was discovered that the model liquid is quite stable at modest temperature and pressures, in agreement with experiment; furthermore, it exhibits a temperature-independent mean inherent structure, as has been found for simpler atomic liquids. However, the imposition of strong compression along with high temperature causes the Si_2F_6 fluid to undergo dissociation, atom exchange, and polymerization reactions. The result of such chemical degradation is a significant shift in the mean inherent structure away from its pure-liquid temperature-independent form.

I. INTRODUCTION

Structural diversity and complexity at the molecular level seem to be characteristic of the liquid state. Their presence complicates the tasks of understanding and predicting the properties of matter in this state. In an effort to bring some conceptual simplification to liquid state theory, we have introduced an "inherent structure" approach,[1-4] and have investigated its applicability to several atomic[5-11] and molecular fluids.[12-16] The present paper concerns the case of liquid Si_2F_6, a substance that is stable in pure form under ordinary temperature and pressure conditions,[17] but can undergo degrading chemical reactions otherwise.[18]

The inherent structure theory resolves the liquid state (or indeed any condensed phase) into a collection of mechanically stable molecular packings, and kinetically induced motions away from those packings. The former are local minima of the system's potential energy function Φ, and are defined to be "the inherent structures." The latter will be largely anharmonic vibrational motions in the cold liquid state, but exhibit an increasingly diffusive character as the temperature rises.

Separation of the pure packing effects from the motional deformations relies upon a natural mapping for the many-body system, a mass-weighted descent on the potential energy hypersurface. Let $\mathbf{R}(t)$ denote the continuous time-dependent configuration vector for the many-body system. If classical mechanics provides an appropriate dynamical description, $\mathbf{R}(t)$ evolves by the Newtonian equations of motion,

$$\mathbf{M}\cdot\ddot{\mathbf{R}}(t) = -\nabla_R\Phi(\mathbf{R}), \tag{1.1}$$

where $\mathbf{M}$ is a diagonal matrix of particle masses. The mass-weighted descent mapping emerges from the first-order version of the Newtonian equations,

$$\mathbf{M}\cdot\dot{R}(u) = -\nabla_R\Phi(\mathbf{R}). \tag{1.2}$$

Excluding certain zero-measure circumstances, the solutions to Eq. (1.2) as virtual time u increases to $+\infty$ will move monotonically downward on the multidimensional Φ hypersurface to a local Φ minimum. In particular, the dynamical trajectory $\mathbf{R}(t)$ can serve as a continuous set of initial ($u = 0$) conditions for integration of Eq. (1.2), and as $u \to +\infty$ generates a record of the Φ minima within whose "basins" the dynamical trajectory travels. This is equivalent to the mapping

$$\mathbf{R}(t) \to \mathbf{R}_q(t) \tag{1.3}$$

from the continuous dynamical trajectory to the discontinuous, piecewise-constant, set of quenched configurations $\mathbf{R}_q$ for the relevant inherent structures.

It should be remarked that the configuration mapping can be carried out either under constant volume or constant pressure conditions.[19] We adhere to the former protocol in the present paper. Under most ordinary circumstances the distinction is expected to be minor.

The conventional, experimentally motivated, means for measuring short-range order in liquids utilizes pair correlation functions.[20] These are found to be temperature-dependent for real and simulated substances, with the magnitude and range of correlation declining with increasing temperature (provided critical points and their neighborhoods are avoided). Previous molecular dynamics simulational studies have revealed that the temperature dependence resides almost exclusively in the motional, rather than packing, aspect of the system, at least for simple atomic and molecular substances. That is, a nearly temperature-independent average inherent structure appears to underlie the liquid state. Measured temperature variations in pair correlation functions reflect the variable extent of intrabasin "vibrational" exploration.

The existence of an accurately temperature-invariant mean inherent structure is clearly violated in cases where the liquid in question can undergo chemical reactions. Two examples that have been studied to date are the thermal polymerization of molecular sulfur (S_8),[13,14] and the high temperature dissociation of fluorine (F_2).[15]

The present study focuses on a polyatomic molecular liquid, Si_2F_6. The objective is to establish the geometric nature of mean inherent structure underlying the liquid phase, and to see if it shares the previously discovered temperature

 0021-9606/91/173614-13$03.00

independence in the absence of chemical reaction.

In Sec. II, we present the model potential employed. In Sec. III we outline the molecular dynamics and configurational mapping protocols. In Sec. IV we display and analyze results from the simulations. Conclusions and related discussion appear in the Sec. V.

II. MODEL POTENTIAL

A properly chosen combination of two-atom and three-atom interaction functions is often sufficient to represent the structures and intramolecular force fields of polyatomic species, as well as interactions between neighboring molecules. Furthermore, no intrinsic distinction is drawn between intramolecular and intermolecular interactions, so that potential Φ is automatically specified in regions of the configuration space corresponding to breakage and reformation of chemical bonds. Atom-exchange, thermal decomposition, and polymerization chemical reactions can all be studied for appropriate substances using this two-atom plus three-atom interaction format.

Such interactions have been derived and exploited previously for systems containing simultaneously both Si and F atoms. The existing applications have been quite different from that required here, specifically they involved interfacial reactions between gaseous fluorine and crystalline silicon.[21,22] However, the component atomic potentials by definition are transferrable to the present case.

Setting $A \equiv$Si and $B \equiv$F for notational simplicity, we have

$$\Phi = \Sigma\, v_{AA} + \Sigma\, v_{AB} + \Sigma\, v_{BB} + \Sigma\, v^{(3)}_{AAA} + \Sigma\, v^{(3)}_{AAB} + \Sigma\, v^{(3)}_{ABB} + \Sigma\, v^{(3)}_{BBB}. \quad (2.1)$$

Roughly speaking, the pair potentials $v_{\alpha\beta}$ are required to produce covalent bonds of the correct strength, length, and stiffness, while the $v^{(3)}_{\alpha\beta\gamma}$ enforce directionality and saturability of those covalent bonds.

The specific two-atom and three-atom functions used for the present study are the set employed in Ref. 22 for simulation of surface chemisorption. An Appendix provides a complete specification for convenience.

An obvious requirement is that the transferrable interactions in Eq. (2.1) should correctly represent the stable molecular structures of at least the simplest silicon fluorides SiF_4 and Si_2F_6. Indeed that is the case. The former is predicted to be tetrahedral, and has no capacity to add a fifth fluorine to the shell of four surrounding the central silicon. The Si_2F_6 molecule produced by the model has (as required) a bond structure analogous to that of ethane (C_2H_6), but with an eclipsed internal conformation. Figure 1 shows the stable structure for the isolated molecule predicted by the model. Its energy is -870.00 kcal/mole compared to the eight free atoms. Bond lengths are 2.506 Å for Si–Si, and 1.660 Å for Si–F, and the F–Si–F angle is 107.6°; these are in reasonable agreement with experiment (2.32 Å, 1.56 Å, and 108.6°, respectively).[23]

Molecular dynamics simulations reported below verify that in the condensed liquid phase with ordinary temperature and pressure conditions the Si_2F_6 molecules retain stability and molecular identity. Preliminary studies established the same for a liquid composed of SiF_4 molecules. The model would have been worthless otherwise. No claim is made that the set of interactions used is optimal for representing the silicon fluorides, and it might be profitable in the future to explore some modifications.

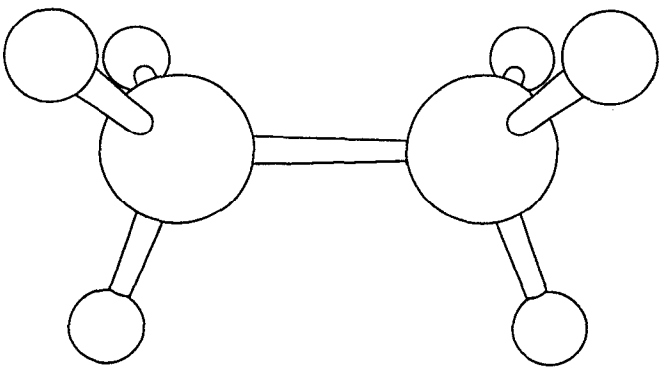

FIG. 1. Molecular structure of an isolated nonvibrating Si_2F_6 molecule predicted by the model interaction.

III. MOLECULAR DYNAMICS PROCEDURE

Our Si_2F_6 simulations have utilized 125 molecules (1000 atoms) residing in a cubic unit cell of appropriate size. Periodic boundary conditions are applied. Coupled Newtonian equations of motion for the system were numerically integrated using a fifth-order predictor–corrector method of Gear.[24] Total energy was accurately conserved during each molecular dynamics run, typically to eight significant figures.

Two liquid densities have been investigated: 1.501 and 1.787 g/cm^3; the corresponding cube edges for the system cell are 28.6572 and 27.0351 Å, respectively, The former is our estimate of the triple point density (occurring experimentally at -18.7 ± 0.1 °C, 780 Torr[17]) based on rough analogies to C_2H_6 and SiF_4, but which unfortunately seems not yet to have been measured. The latter is a highly compressed state with linear dimensions reduced by factor 1.06 compared to the triple-point estimate.

In order to initiate the molecular dynamics simulation, intact Si_2F_6 molecules were placed in a regular cubic array within an expanded cell. The atoms were given small random velocities. A series of preparative molecular dynamics runs was carried out; between each pair of runs the density was increased slightly and kinetic energy uniformly reduced (by velocity scaling), until finally the desired density and temperature was attained. During "production runs" at fixed density the numerical integration proceeded with step length

$$\Delta t = 0.004\tau, \quad (3.1)$$

where τ is a natural time unit determined by the mass (m), and the pair-interaction length (σ) and energy (ϵ) parameters for Si,[10]

$$\tau = \sigma(m/\epsilon)^{1/2} = 7.6634 \times 10^{-14}\ \text{s}. \quad (3.2)$$

One of the ancillary objectives of this project has been to

determine the extent to which the collection of model Si_2F_6 molecules would remain stable over typical molecular dynamics time scales (10^{-12} to 10^{-9} s) while subject to extremes of temperature and pressure. Covalent bond connectivity has been our means of monitoring stability or, in its absence, identifying the new chemical species that have formed. For this purpose we define a pair of atoms to be covalently bonded if their separation r_{ij} does not exceed four-thirds of the equilibrium bond length for that pair. The specific cutoffs thus applied are as follows:

$$\begin{aligned} &\text{Si–Si: } \tfrac{4}{3}(2.3517\ \text{Å}) = 3.1356\ \text{Å}, \\ &\text{Si–F: } \tfrac{4}{3}(1.6011\ \text{Å}) = 2.1348\ \text{Å}, \\ &\text{F–F: } \tfrac{4}{3}(1.4349\ \text{Å}) = 1.9132\ \text{Å}. \end{aligned} \tag{3.3}$$

In a few instances, regularly spaced (in time) configurations of the system were stored for later mapping onto potential energy minima. This mapping was effected by the MINOP procedure.[25] Averaged inherent structures determined this way for the liquid are reported and discussed below.

IV. INHERENT STRUCTURES

A. Low density results

When the Si_2F_6 system is maintained at density 1.501 g/cm^3, we find that heating and cooling over a wide temperature range does not produce chemical degradation over the time scale of molecular dynamics. Figure 2 illustrates the point by showing observed values of mean potential energy for the system between approximately 450 and 2000 K. Separate data points in the plot represent runs of length $10^4\Delta t$ (3.065 ps), and were obtained during both heating and cooling sequences. Aside from minor statistical fluctuations the points display a smooth and reproducible trend. Slight upward curvature is present reflecting increasing anharmonicity as the temperature rises, and this implies a rise in constant-volume heat capacity with temperature.

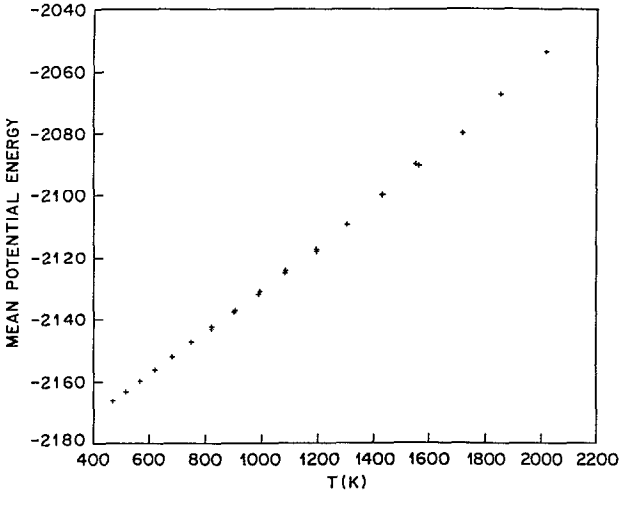

FIG. 2. Mean potential energy vs absolute temperature for 125 Si_2F_6 molecules at 1.501 g/cm^3.

The bond monitoring procedure indeed verifies that all 125 molecules remain intact during heating and cooling. At the lower temperatures all expected covalent bonds (and no others) are present at every instant of observation. Vigorous thermal vibrations at the high temperature extreme cause some bonds (particularly those of type Si–F) momentarily to exceed the counting thresholds, but these events are rare, transitory, and not accompanied by irreversible chemical change.

Figures 3(a)–3(i) present atomic pair correlation functions for a relatively low-temperature thermodynamic state, 470 K. Three kinds of atom pairs are present: FF, SiF, and SiSi, and Figs. 3(a)–3(c) show the total pair correlation functions for each. These total functions can be resolved into "intramolecular" and "intermolecular" parts, where the former represents pairs of atoms initially present in the same molecule, the latter those pairs initially present in different molecules. Figures 3(d)–3(f) show only the "intermolecular" contributions, while Figs. 3(g)–3(i) display only the "intramolecular" contributions. This last triplet presents patterns expected from the molecule shown in Fig. 1, subject to modest vibrational motion and hindered internal rotation about the Si–Si bond.

Figures 4(a)–4(i) present the same set of atomic pair correlation functions at the significantly higher temperature 1720 K, but still at density 1.501 g/cm^3. The influence of temperature rise is substantial and as expected. A comparison of corresponding functions from the two sets shows that both intramolecular and intermolecular features are considerably broadened, lowered, and rendered less distinctive at elevated temperature.

Average inherent structures have been determined for each of the two thermodynamic states represented in Figs. 3 and 4. Twenty-one system configurations, equally spaced in time, were mapped onto the relevant potential minima, as described in the Introduction for each temperature. The mean values of the quenched-configuration potential Φ_q were quite close,

$$\begin{aligned} \langle \Phi_q \rangle &= -2195.9577 \text{ (from 470 K)}, \\ &= -2193.8748 \text{ (from 1720 K)}. \end{aligned} \tag{4.1}$$

The potential minima contributing to these averages were each narrowly distributed in energy (rms deviations $\cong 0.11$ and 0.34, respectively), but in fact were all distinct.

Inherent pair correlation functions, determined as averages over the respective sets of 21 potential minima, are displayed in Figs. 5(a)–5(i) for the lower temperature thermodynamic state, and in Figs. 6(a)–6(i) for the higher temperature thermodynamic state.

Compared to the prequench pair correlation functions, the data bases from which Figs. 5 and 6 were prepared are relatively small. Consequently the quench pair correlation functions are relatively "noisy." This situation results from the fact that locating minima in many-body strongly interacting systems is numerically a very demanding task relative to the integration of Newton's dynamical equations. But in spite of this difficulty a clear message emerges from Figs. 5 and 6. Not only has the quenching (mapping to potential minima) substantially sharpened the image of short-range

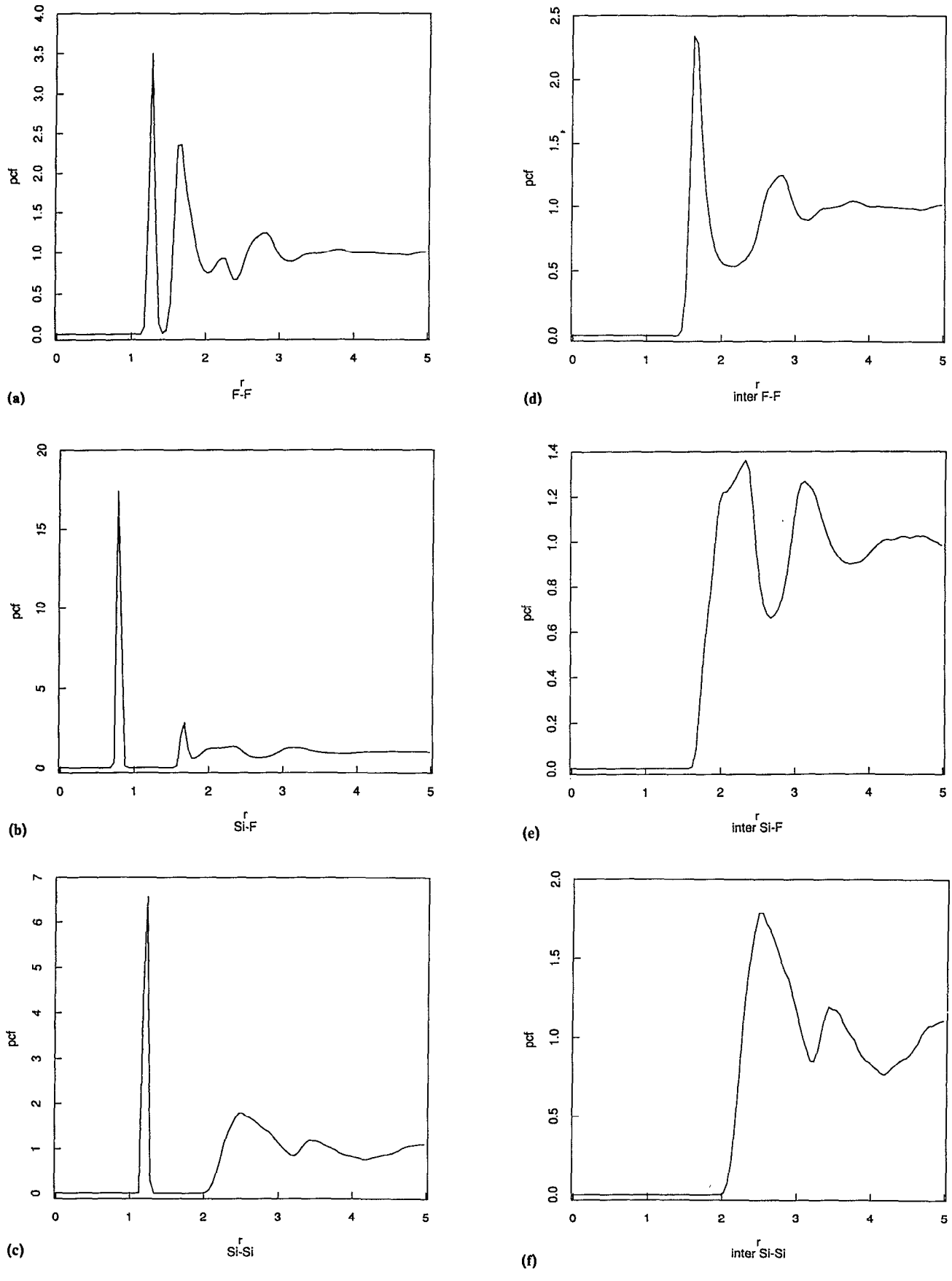

FIG. 3. Atomic pair correlation functions for Si_2F_6 at 1.501 g/cm^3 and 470 K; (a) total F–F, (b) total Si–F, (c) total Si–Si, (d) intermolecular F–F, (e) intermolecular Si–F, (f) intermolecular Si–Si, (g) intramolecular F–F, (h) intramolecular Si–F, and (i) intramolecular Si–Si. The distance unit is $\sigma(\mathrm{Si}) = 2.0951$ Å.

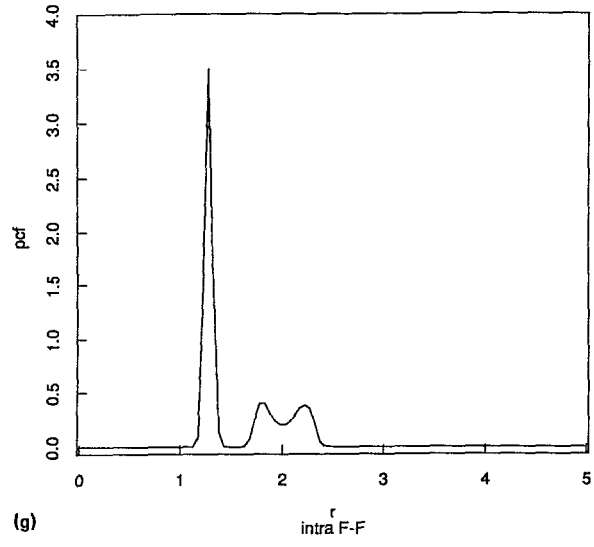

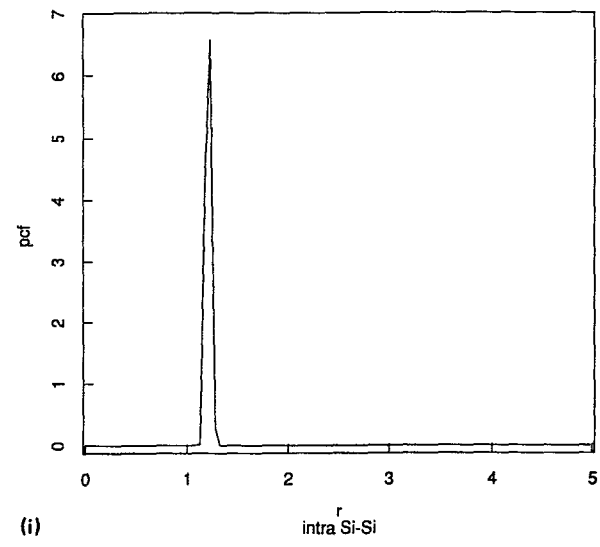

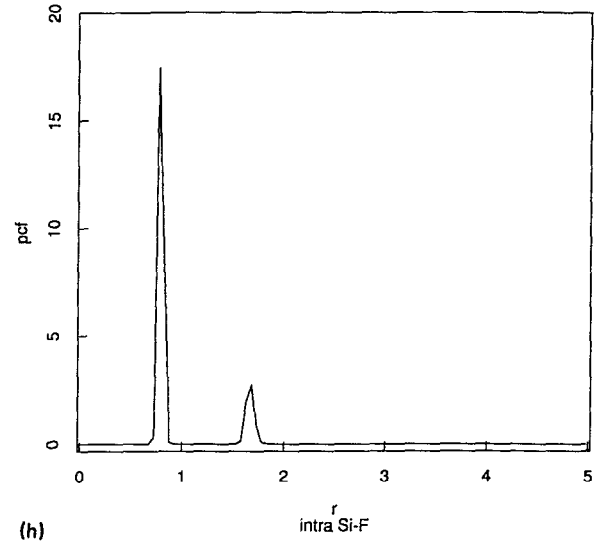

FIG. 3. (*Continued.*)

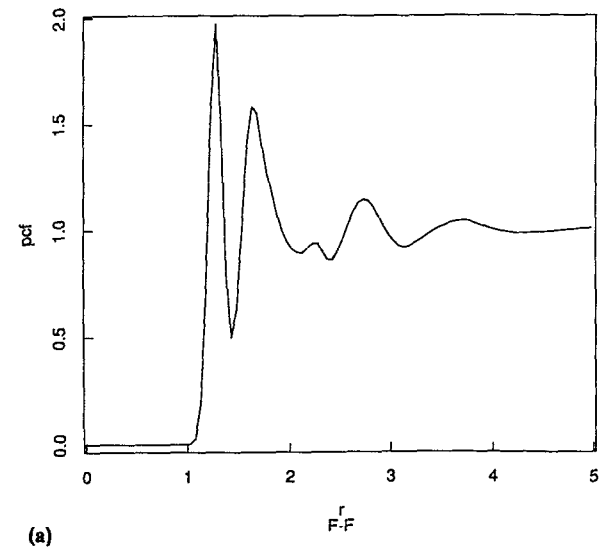

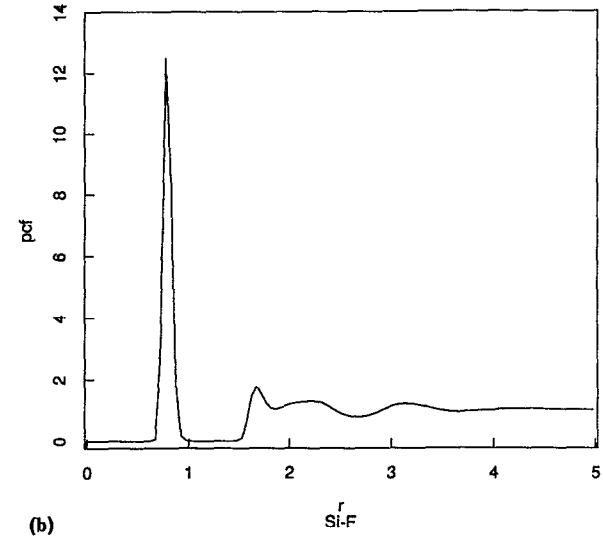

FIG. 4. Atomic pair correlation functions for Si_2F_6 at 1.501 g/cm^3 and 1720 K; (a) total F–F, (b) total Si–F, (c) total Si–Si, (d) intermolecular F–F, (e) intermolecular Si–F, (f) intermolecular Si–Si, (g) intramolecular F–F, (h) intramolecular Si–F, and (i) intramolecular Si–Si.

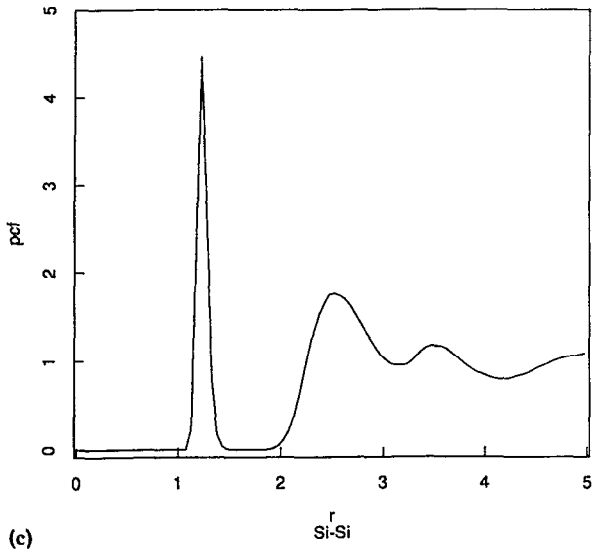

(c)

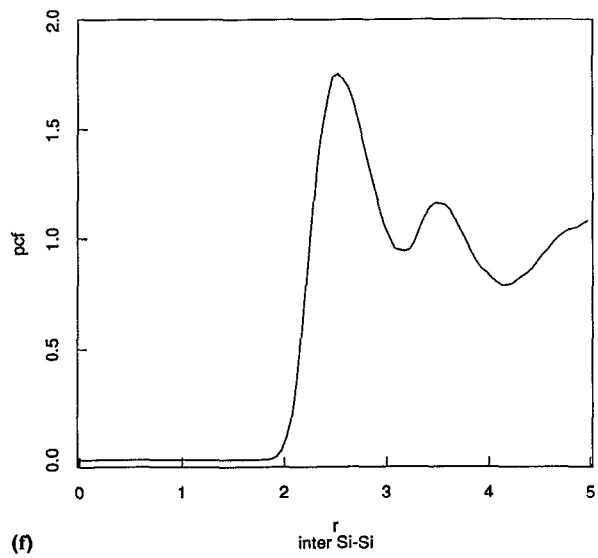

(f)

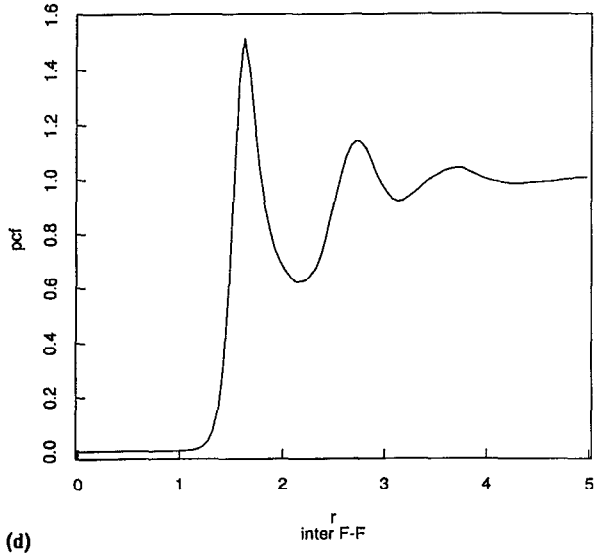

(d)

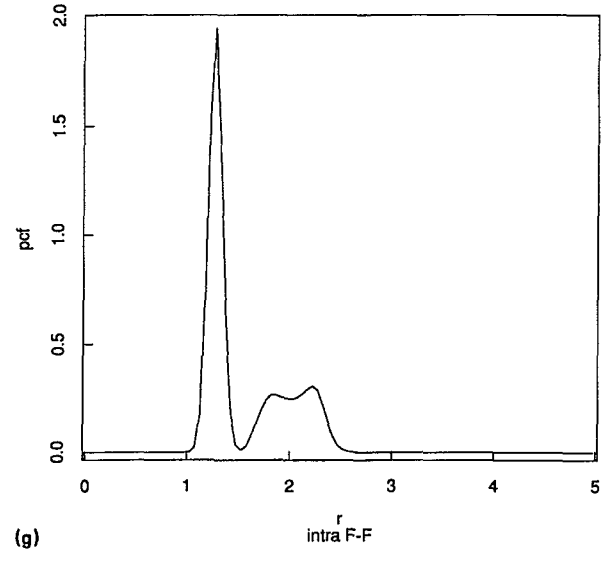

(g)

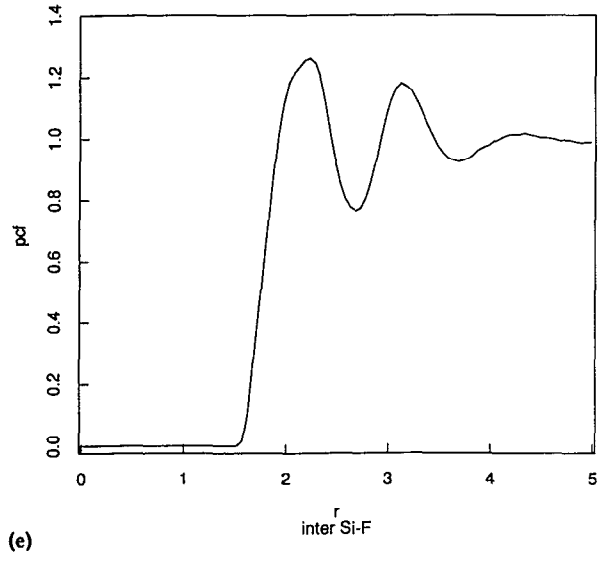

(e)

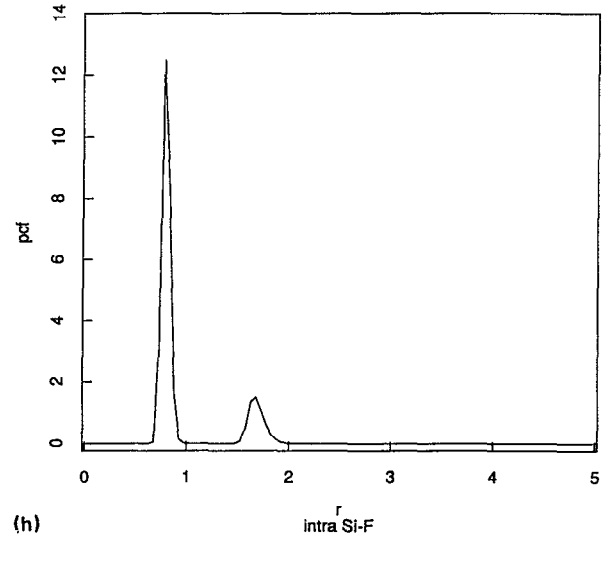

(h)

FIG. 4. (*Continued.*)

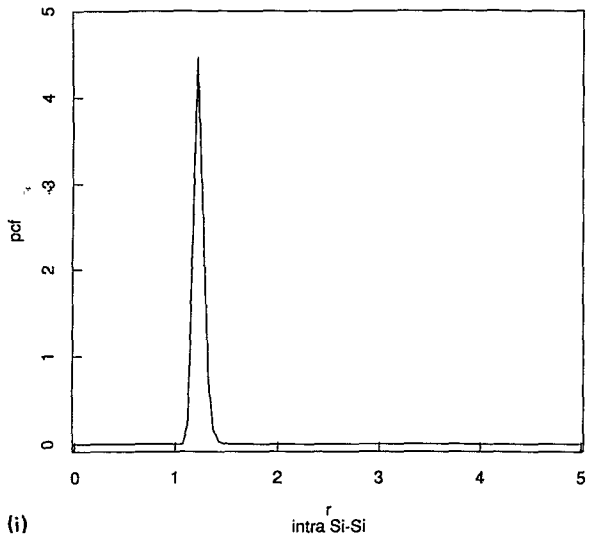

FIG. 4. (*Continued.*)

order in the system, but, also, that sharpened image is virtually the same whether from low or from high temperature thermodynamic states. By comparing corresponding functions from the figure sets (Figs. 3–6) it is clear that the mapping to minima effectively neutralizes the smearing influence of thermal motions. Evidently Si_2F_6 provides yet another example (at least in its region of chemical stability) of the existence of a nearly temperature-independent inherent structure underlying the dense fluid states.

Structural information present in the average inherent structure functions, Figs. 5 and 6, can only be interpreted in terms of amorphous deposits. Neighboring molecules are arranged so as to yield substantial short-range order, but sufficient local packing diversity is present to eliminate long-range order. Neighbor forces have rather little influence on covalent bond length distributions within molecules. However, it is evident from the larger-distance components of the intramolecular F–F correlations [Figs. 5(g) and 6(g)] that typical inherent structures lock Si_2F_6 molecules into a continuum of internal rotational configurations.

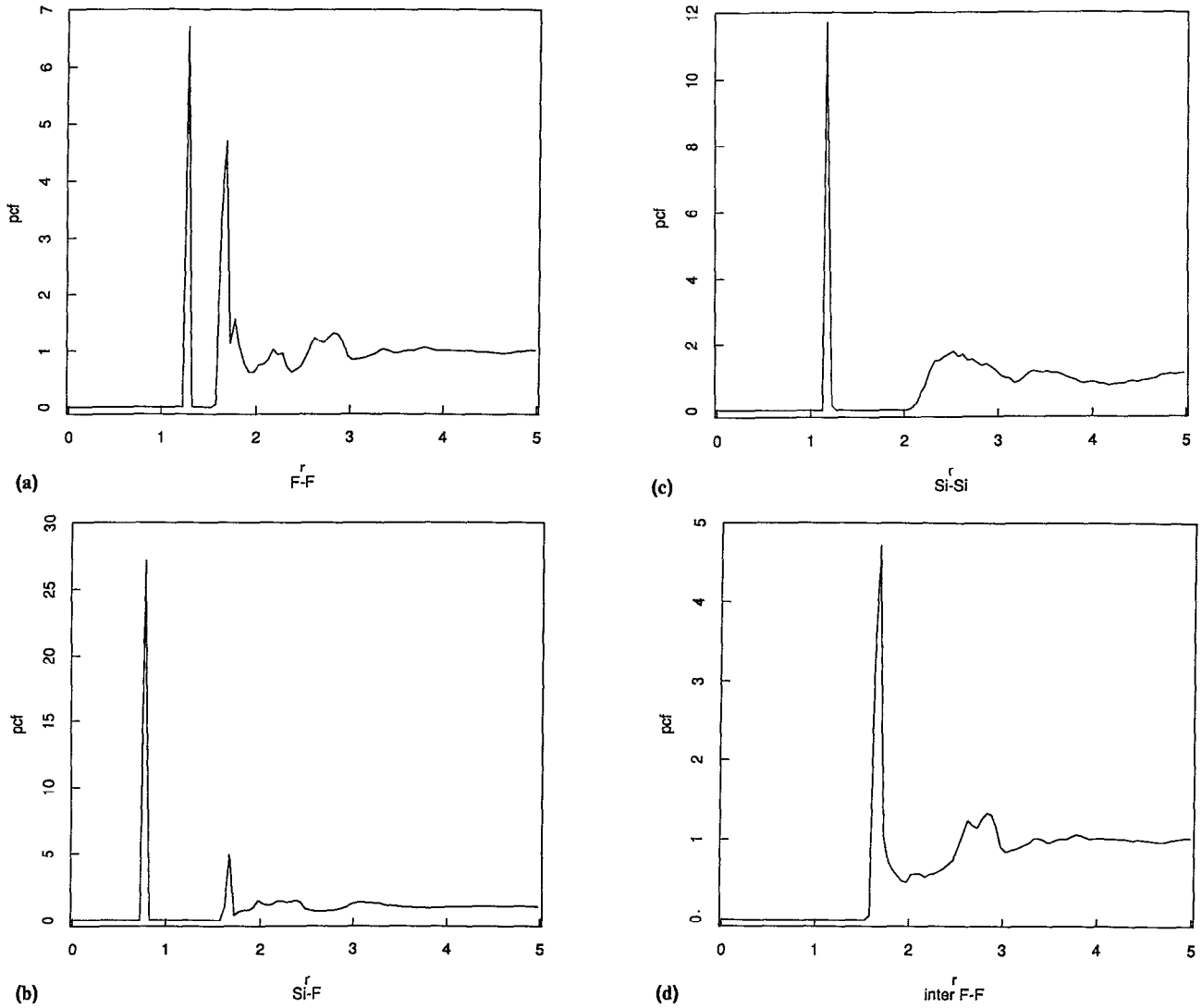

FIG. 5. Averaged-inherent-structure pair-correlation functions for the thermodynamic state 1.501 g/cm^3, 470 K. Cases (a)–(i) are arranged as in Figs. 3 and 4.

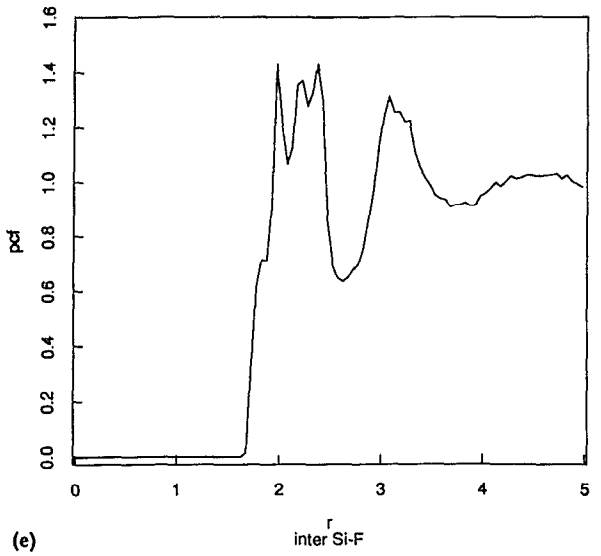

(e)

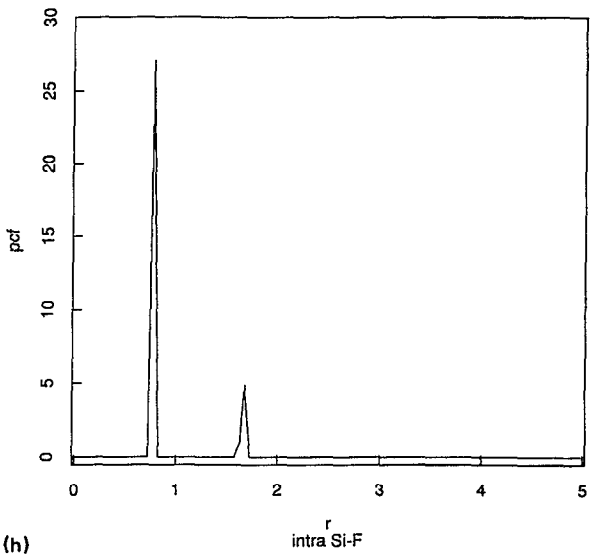

(h)

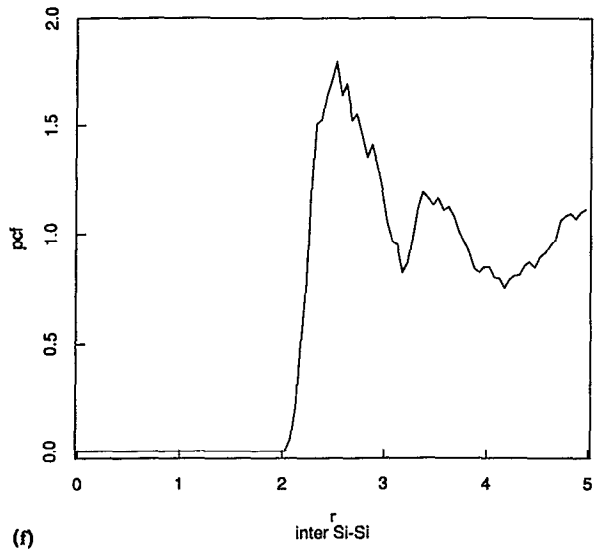

(f)

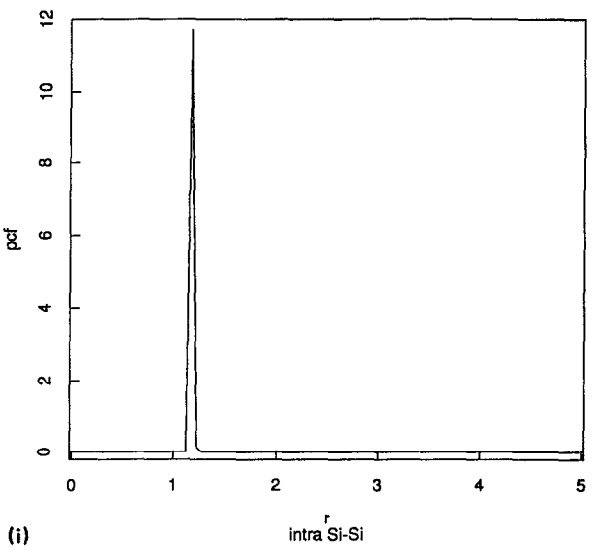

(i)

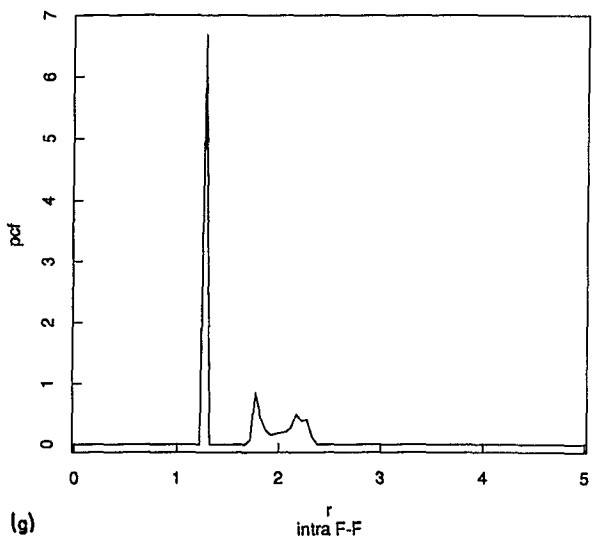

(g)

FIG. 5. (*Continued.*)

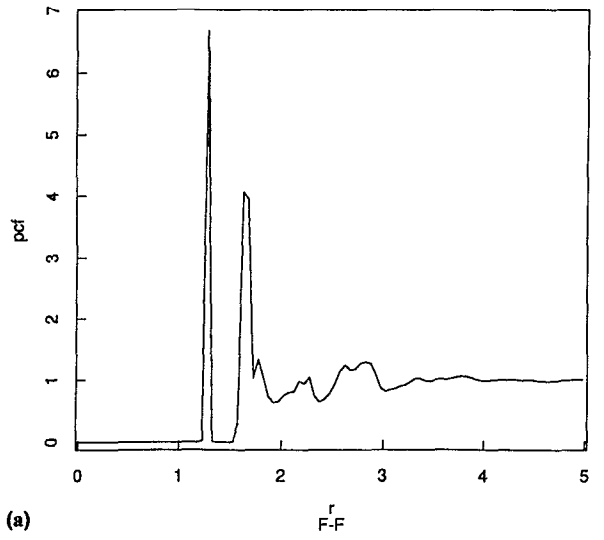

(a)

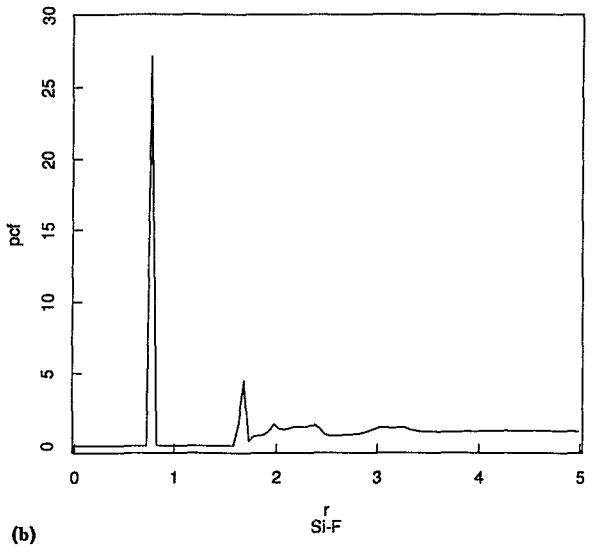

(b)

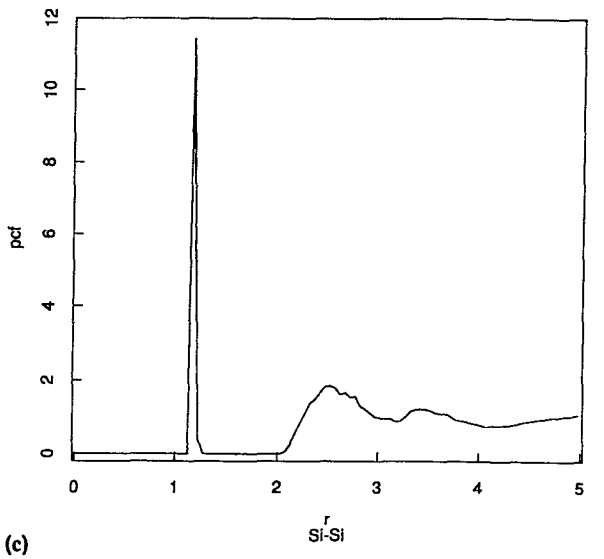

(c)

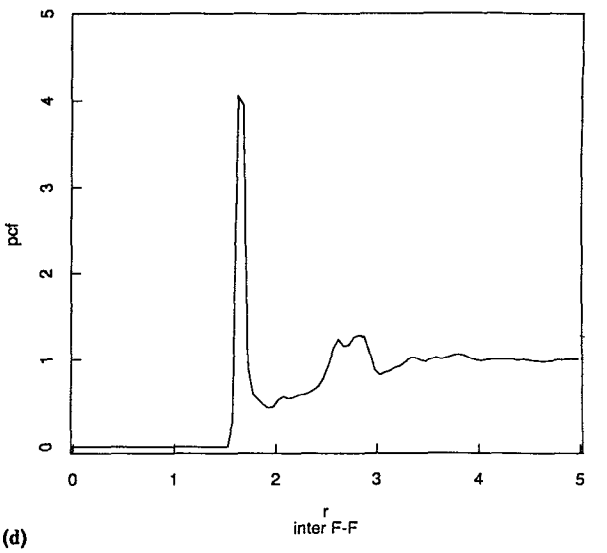

(d)

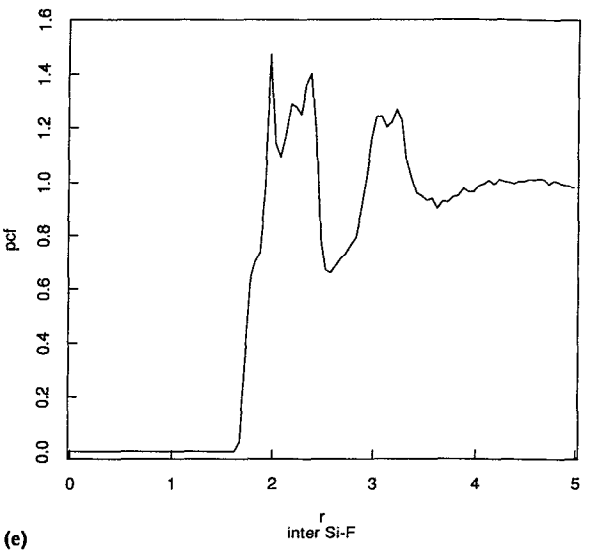

(e)

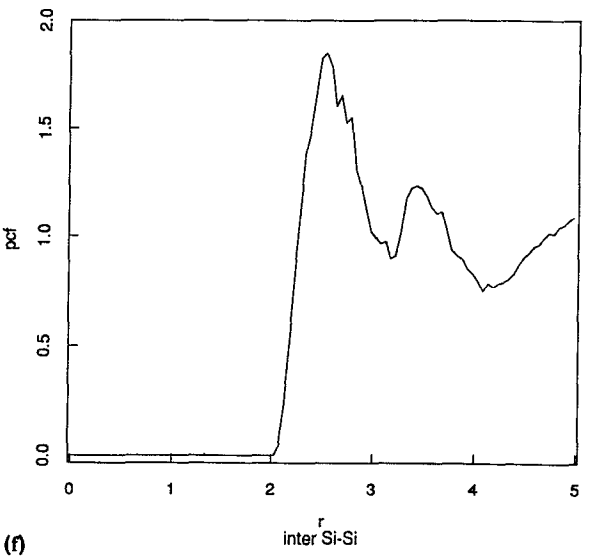

(f)

FIG. 6. Averaged-inherent-structure pair-correlation functions for the thermodynamic state 1.501 g/cm^3, 1720 K. Cases (a)–(i) are arranged as *in* Figs. 3–5.

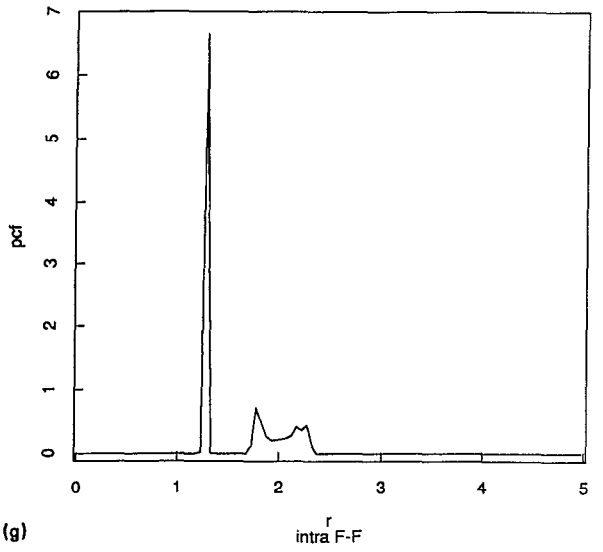

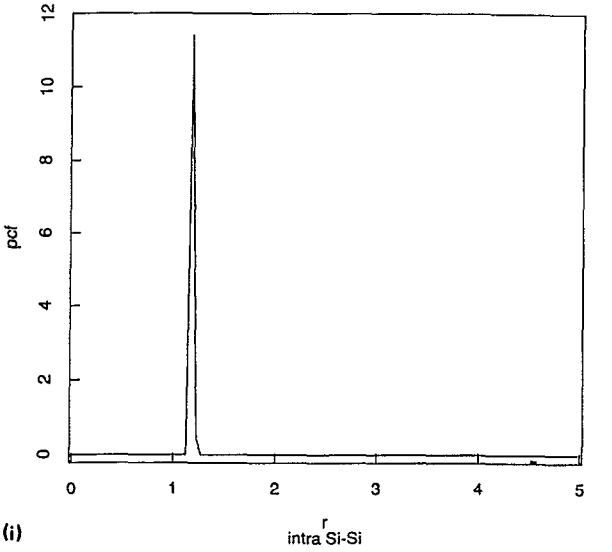

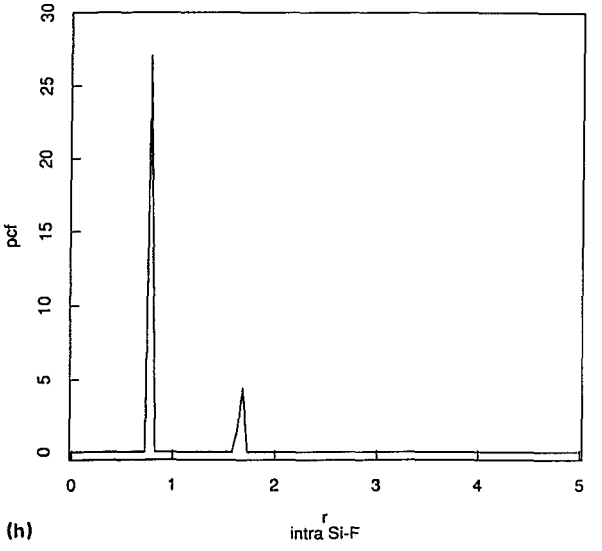

FIG. 6. (*Continued.*)

B. High density results

Heating the Si_2F_6 system at the higher density 1.787 g/cm^3 produces irreversible chemical change. Figure 7 shows the record of mean potential energy for the system during a molecular dynamics sequence that began at approximately 150 K, carried the system stepwise to approximately 3400 K, then brought it back to relatively low temperature (480 K). The failure of heating and cooling branches to superpose is connected to the chemical transformations.

The final system configuration encountered at the end of the heating–cooling sequence was mapped onto its relevant potential energy minimum by the usual procedure, since it has been discovered before that this is a potent tool for analyzing chemical species present in dense amorphous media.[26,27] Application of the pair bonding criteria (3.3) to the resulting single inherent structure produced shows the presence of a complex mixture of species; these are listed in Table I. Because of the high pressure and poor packing of atoms it is not surprising that species such as Si_2F_8, and

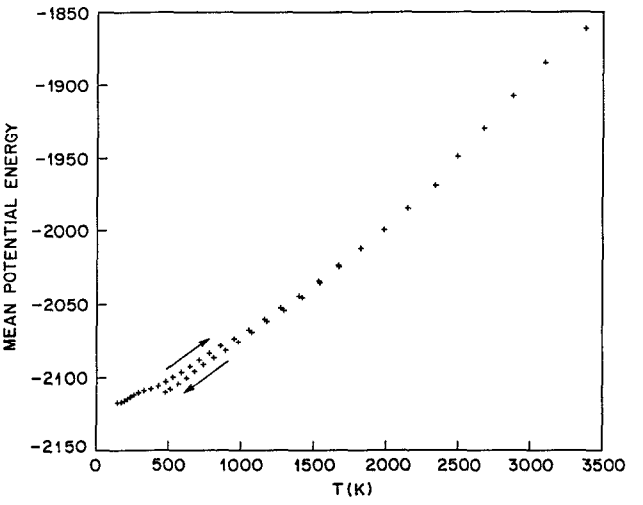

FIG. 7. Mean potential energy vs absolute temperature for the system at 1.787 g/cm^3. The initial state consisted of 125 intact Si_2F_6 molecules.

TABLE I. Chemical species in the inherent structure of the strongly heated, high density system.

Molecule	Number of occurrences
SiF_3	27
SiF_4	67
Si_2F_4	1
Si_2F_5	12
Si_2F_6	17
Si_2F_8	2
Si_3F_6	1
Si_3F_7	6
Si_3F_8	11
Si_4F_6	1
Si_4F_9	2
Si_4F_{10}	1
Si_4F_{12}	1
Si_5F_9	1
Si_5F_{11}	1
Si_5F_{17}	1

Si_4F_{12}, formally violating the usual valence rules, might infrequently be encountered. Careful examination of bonding patterns reveal that these species contain "divalent" fluorine bridges, a structural feature not observed in the low-density calculations.

The chemical transformations clearly influence the atomic pair correlation functions. This is most obvious when examining the "intramolecular" components for the single inherent structure just discussed. Specifically, these are pairs that resided in the same Si_2F_6 molecule before the destructive heating and cooling sequence, but that often are found in distinct molecules afterward. Figures 8(a)–8(c) present these three intramolecular correlation functions, showing indeed that some pairs have become chemically unlinked and have drifted apart.

Figures 9 and 10 illustrate the influence that chemical transformations can exert on the inherent structures, in violation of the temperature independence of average inherent structure observed when the system consists only of Si_2F_6 species. The first of these, Fig. 9, shows the total Si pair correlation function averaged over 21 inherent structures for the intact Si_2F_6 compressed fluid (1.787 g/cm^3) at 479 K. The second, Fig. 10, shows the same quantity after the constant-density heating and cooling treatment (Fig. 7), evaluated for the single inherent structure at the end of the treatment (prequench temperature 338 K). Before reaction the sharp intramolecular peak is well separated from the larger-distance intermolecular pairs by a wide gap; reaction causes substantial filling of the gap and a reduction in the height of the intramolecular peak. The other correlation functions also exhibit substantial reaction-induced changes.

V. CONCLUSIONS

Three principal conclusions emerge from the present study.

(1) The silicon fluorides, particularly Si_2F_6, can be chemically modeled with a linear combination of transferrable two-atom and three-atom potential functions. The resulting

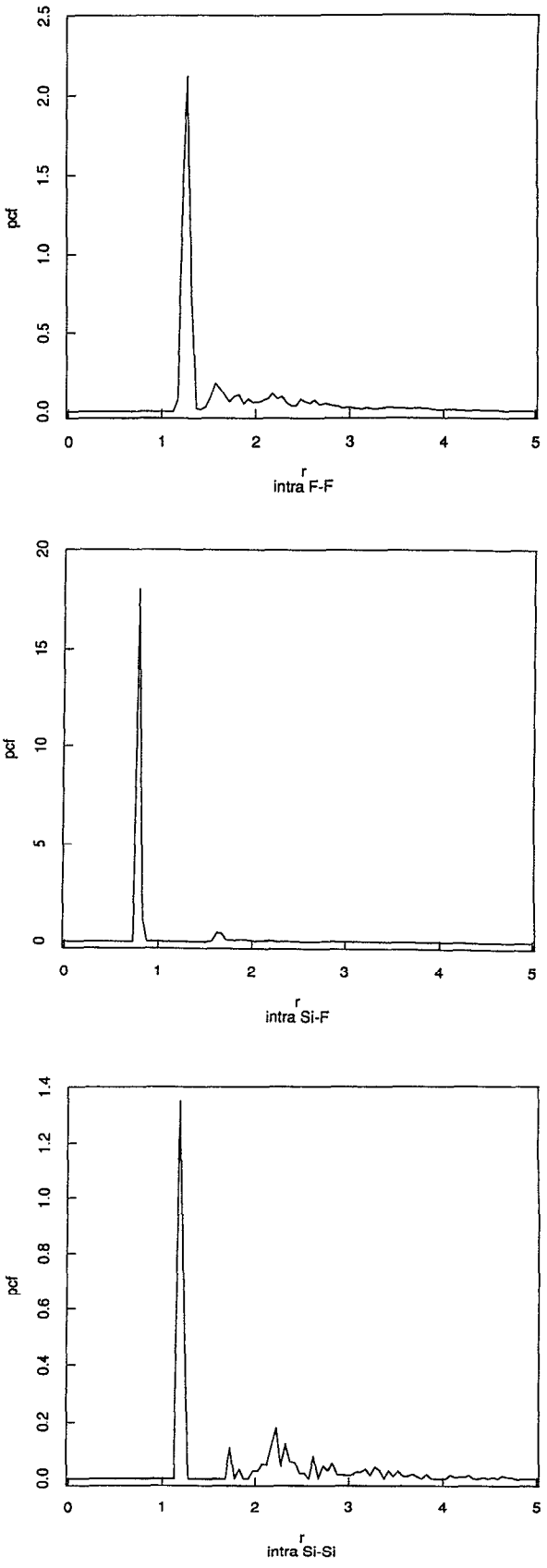

FIG. 8. Atomic pair correlations in a single inherent structure, for pairs initially bound within the same Si_2F_6 molecule. The system is at the higher density 1.787 g/cm^3, and has been transformed chemically by the heating and cooling sequence indicated in Fig. 7.

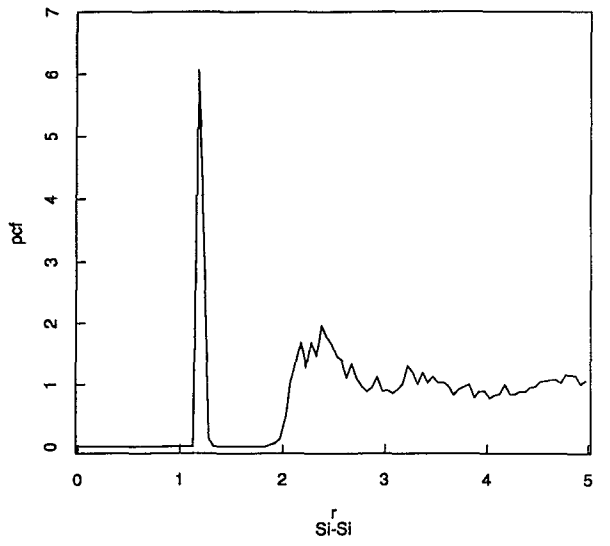

FIG. 9. Inherent structure pair correlation for silicon atoms in the unreacted Si_2F_6 system at 1.787 g/cm^3.

molecules are stable in condensed phases at ordinary temperature and pressure, but undergo a variety of chemical reactions under more extreme conditions, exhibiting dissociation, atom exchange, and polymerization.

(2) If temperature and pressure conditions are such that chemical reactions do not occur, liquid Si_2F_6 exhibits a temperature-independent average inherent structure. This was made clear by examining atom-pair correlation functions before and after mapping liquid-phase configurations onto potential energy minima by mass-weighted descent, Eq. (1.2). Temperature dependence of short-range order arises almost exclusively from intrabasin thermal excitation (anharmonic and diffusionally interrupted vibrations). In this respect the polyatomic Si_2F_6 behaves in a manner similar to several simple atomic cases that have been examined before by computer simulation coupled to mapping onto potential minima.

(3) When harsh conditions lead to chemical degradation of the initially pure Si_2F_6 medium, the average inherent structure indeed does change, showing consequently a chemically induced temperature dependence. In these circumstances the mass-weighted descent mapping provides a convenient and powerful tool for monitoring the survival of Si_2F_6 molecules and the appearance of new species.

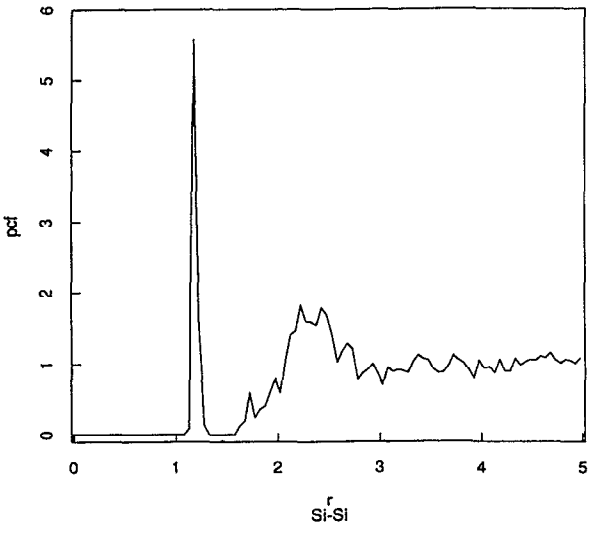

FIG. 10. Inherent structure pair correlation for silicon atoms in the 1.787 g/cm^3 system after thermally induced chemical degradation.

APPENDIX

Adhering to the convention that $A \equiv$ Si and $B \equiv$ F, and using Si-based length and energy units,[10]

$$\sigma = 2.0951 \text{ Å},$$

$$\epsilon = 3.4723 \times 10^{-12} \text{ erg/atm} = 50.0 \text{ kcal/mole}, \tag{A1}$$

the pair potentials employed are the following:

$$v_{AA}(r) = 7.049\,556\,277(0.602\,224\,558 r^{-4} - 1) \times \exp[(r-1.8)^{-1}] \quad (0<r<1.8), \tag{A2}$$
$$= 0 \quad (1.8 \leqslant r);$$

$$v_{AB}(r) = 21.234\,141\,38(0.569\,547\,643 r^{-3} - r^{-2}) \times \exp[1.3(r-1.8)^{-1}] \quad (0<r<1.8), \tag{A3}$$
$$= 0 \quad (1.8 \leqslant r);$$

$$v_{BB}(r) = 0.522\,76(0.112\,771 r^{-8} - r^{-4}) \times \exp[0.579\,495/(r-2.086\,182)] \quad (0<r<2.086\,182),$$
$$= 0 \quad (2.086\,182 \leqslant r). \tag{A4}$$

Each of these functions has derivatives of all orders vanishing at the "cutoff" point beyond which it becomes identically zero.

The three-atom interactions $v^{(3)}_{XYZ}$ (X, Y, $Z = A$ or B) are expressed as linear combinations of triangle vertex functions,

$$v^{(3)}_{XYZ}(\mathbf{r}_X,\mathbf{r}_Y\mathbf{r}_Z) = h_{XYZ}(r_{YX},r_{YZ},\theta_Y) + h_{YXZ}(r_{XY},r_{XZ},\theta_X) + h_{XZY}(r_{ZX},r_{ZY},\theta_Z); \tag{A5}$$

here, for instance, θ_Y is the angle at atom (vertex) Y subtended by X and Z at respective distances r_{XY} and r_{YZ}.

There are six distinct triangle vertex functions for the present case with two atomic species. Each exhibits smooth cutoff behavior analogous to that of the two-atom interactions, when either of its scalar distance variables passes through an essentially singular point of the small distance component functional form. These latter are the following:

$$h_{AAA}(r,s,\theta) = 21 \exp\{1.2[(r-1.8)^{-1} + (s-1.8)^{-1}]\} \times (\cos\theta + \tfrac{1}{3})^2, \tag{A6}$$

$$h_{AAB}(r,s,\theta) = 15 \exp[(r-1.8)^{-1} + (s-1.8)^{-1}] \times (\cos\theta + \tfrac{1}{3})^2, \tag{A7}$$

$$h_{ABA}(r,s,\theta) = 50\exp\{1.3[(r-1.8)^{-1}+(s-1.8)^{-1}]\}, \quad \text{(A8)}$$

$$h_{BAB}(r,s,\theta) = [24(\cos\theta - \cos 103°)^2 - 3.2] \times \exp[(r-1.8)^{-1}+(s-1.8)^{-1}], \quad \text{(A9)}$$

$$h_{ABB}(r,s,\theta) = 3.5\exp[(r-1.8)^{-1}+(s-1.8)^{-1}], \quad \text{(A10)}$$

$$h_{BBB}(r,s,\theta) = 0.081\,818\,2(rs)^{-4}\exp\{0.579\,495\,[(r-2.086\,182)^{-1}+(s-2.086\,182)^{-1}]\} + (38.295 - 19.1475\cos^2\theta)\exp\{1.738\,485[(r-1.622\,586)^{-1}+(s-1.622\,586)^{-1}]\}. \quad \text{(A11)}$$

[1] F. H. Stillinger and T. A. Weber, Kinam **3A**, 159 (1981).
[2] F. H. Stillinger and T. A. Weber, Phys. Rev. A **25**, 978 (1982).
[3] F. H. Stillinger and T. A Weber, Phys. Rev. A **28**, 2408 (1983).
[4] F. H. Stillinger and T. A. Weber, Science **228**, 983 (1984).
[5] T. A. Weber and F. H. Stillinger, J. Chem. Phys. **80**, 2742 (1984).
[6] F. H. Stillinger and T. A. Weber, J. Chem. Phys. **80**, 4434 (1984).
[7] T. A. Weber and F. H. Stillinger, J. Chem. Phys. **81**, 5089 (1984).
[8] F. H. Stillinger and T. A. Weber, J. Chem. Phys. **81**, 5095 (1984).
[9] T. A. Weber and F. H. Stillinger, Phys. Rev. B **31**, 1954 (1985).
[10] F. H. Stillinger and T. A. Weber, Phys. Rev. B **31**, 5262 (1985). Phys. Rev. B **33**, 1451 (1986).
[11] T. A. Weber and F. H. Stillinger, Phys. Rev. B **32**, 5402 (1985).
[12] F. H. Stillinger and T. A. Weber, J. Phys. Chem. **87**, 2833 (1983).
[13] F. H. Stillinger, T. A. Weber, and R. A. LaViolette, J. Chem. Phys. **85**, 6460 (1986).
[14] F. H. Stillinger and T. A. Weber, J. Phys. Chem. **91**, 4899 (1987).
[15] F. H. Stillinger and T. A. Weber, J. Chem. Phys. **88**, 5123 (1988).
[16] L. J. Root and F. H. Stillinger, J. Chem. Phys. **90**, 1200 (1989).
[17] *Gmelins Handbuch der Anorganischen Chemie. Silicium*, Teil B, System-Nummer 15, edited by E. H. E. Pietsch (Verlag Chemie GMBH, Weinheim/Bergstrasse, 1959), pp. 633–635.
[18] R. L. Jenkins, A. J. Vanderwielen, S. R. Ruis, S. R. Gird, and M. A. Ring, Inorg. Chem. **12**, 2968 (1973).
[19] F. H. Stillinger, Phys. Rev. B **41**, 2409 (1990).
[20] J. P. Hansen and I. R. McDonald, *Theory of Simple Liquids*, 2nd ed. (Academic, New York, 1986).
[21] F. H. Stillinger and T. A. Weber, Phys. Rev. Lett. **62**, 2144 (1989).
[22] T. A. Weber and F. H. Stillinger, J. Chem. Phys. **92**, 6239 (1990).
[23] H. Oberhammer, J. Mol. Struct. **31**, 237 (1976).
[24] C. W. Gear, *Numerical Initial Value Problems in Ordinary Differential Equations* (Prentice–Hall, Englewood Cliffs, NJ, 1971).
[25] L. C. Kaufmann (private communication).
[26] F. H. Stillinger, in *Statphys* 16, edited by H. E. Stanley (North-Holland, Amsterdam, 1986), pp. 142–149.
[27] T. A. Weber and F. H. Stillinger, J. Chem. Phys. **87**, 3252 (1987).